Multifractality of eigenfunctions in spin chains

Y. Y. Atas and E. Bogomolny
Université Paris-Sud, CNRS, LPTMS, UMR8626, 91405 Orsay, France
(Received 21 May 2012; published 3 August 2012)

We investigate different one-dimensional quantum spin-$\frac{1}{2}$ chain models, and by combining analytical and numerical calculations we prove that their ground state wave functions in the natural spin basis are multifractals with, in general, nontrivial fractal dimensions.

DOI: 10.1103/PhysRevE.86.021104 PACS number(s): 05.50.+q, 75.10.Jm, 75.10.Pq

I. INTRODUCTION

One-dimensional quantum spin chains are among the oldest and most investigated fundamental models in physics. Introduced as toy models of magnetism [1], they quickly became a paradigm of quantum integrable models (see, e.g., [2–5]). A prototypical example is the XYZ Heisenberg model [1] for N spins-$\frac{1}{2}$ in external fields with periodic boundary conditions,

$$\mathcal{H} = -\sum_{n=1}^{N}\left[\frac{1+\gamma}{2}\sigma_n^x\sigma_{n+1}^x + \frac{1-\gamma}{2}\sigma_n^y\sigma_{n+1}^y + \frac{\Delta}{2}\sigma_n^z\sigma_{n+1}^z + \lambda\sigma_n^z + \alpha\sigma_n^x\right], \quad (1)$$

and its various specifications for different values of parameters. $\sigma_n^{x,y,z}$ are the Pauli matrices at site n.

In the natural basis of z components of each spin, $|\vec{\sigma}\rangle = |\sigma_1,\ldots,\sigma_N\rangle$, where $\sigma_j = \pm 1$, any Hamiltonian of N spins-$\frac{1}{2}$ is represented by an $M \times M$ matrix with dimension $M = 2^N$. Many different methods were developed to determine the exact spectra of such matrices [2–5]. The calculation of eigenfunctions is more involved. A wave function of N spins-$\frac{1}{2}$ in the spin-z basis can be written as

$$\Psi = \sum_{\vec{\sigma}} \Psi_{\vec{\sigma}}|\vec{\sigma}\rangle, \quad (2)$$

where the summation is taken over all $M = 2^N$ configurations with $\sigma_j = \pm 1$. In general, coefficients $\Psi_{\vec{\sigma}}$ can be found only after the matrix diagonalization, which for large N is a hard numerical problem. Even in integrable cases, eigenfunctions of spin chains look erratic (cf. the figures below) and their structure is not well understood.

The purpose of this article is to prove that ground state (GS) wave functions for different one-dimensional spin chain models are multifractals in the spin-z basis.

II. MULTIFRACTALITY

Multifractality is a general notion introduced to characterize quantitatively irregular structures appearing in different problems, such as turbulence, dynamical systems, geophysics, etc. [6–8]. Wave function multifractality attracted wide attention when it was recognized that it appears at the point of the metal-insulator transition (MIT) in the three-dimensional Anderson model [9] (cf. [10]).

For eigenfunctions such as that in (2), one uses the following definition (cf. [10]). Let $S_R(q,M)$ be the Rényi entropy for an eigenfunction (2) of a matrix of finite size M,

$$S_R(q,M) = -\frac{1}{q-1}\ln\left(\sum_{\vec{\sigma}}|\Psi_{\vec{\sigma}}|^{2q}\right), \quad (3)$$

with normalized coefficients $\Psi_{\vec{\sigma}}$, $\sum_{\vec{\sigma}}|\Psi_{\vec{\sigma}}|^2 = 1$.

Fractal dimensions, D_q, are defined from the behavior of the Rényi entropy (3) in the limit $M \to \infty$ [10],

$$D_q = \lim_{M\to\infty}\frac{S_R(q,M)}{\ln M}. \quad (4)$$

The case in which D_q is a nonlinear function of q corresponds to a multifractal irregular behavior.

Fractal dimensions (4) give a concise description of eigenfunction moments in the limit of large dimensionality of the Hilbert space and serve as simple indicators of wave function spreading in different scales. The multifractal formalism is especially important in many-body problems where an exponentially large number of components renders the investigation difficult and not transparent. It seems that the notion of multifractality in many-body problems was overlooked in previous studies. For example, the Rényi and Shannon entropies are calculated for GS wave functions of certain spin chains in [11–14], but terms linear in $\ln M$ which determine D_q in (4) were regularly ignored and only next-to-leading terms have been investigated, as is usual in conformal field theories. To the best of our knowledge, only a recent paper [15] briefly mentioned the existence of multifractality in a spin model.

The simplest method to find fractal dimensions is the direct numerical calculation of the GS wave function for a different number of spins and a subsequent extrapolation of the Rényi entropy for large M. Definition (4) is well suited for positive q. For many problems (but not for all), fractal dimensions can be calculated also for negative q [16,17]. Of course, if certain coefficients in (2) are zero due to an exact symmetry, they are not included in the calculation of the Rényi entropy (3) for $q \leqslant 0$.

In what follows, we investigate various specifications of the Heisenberg model (1), and by combining numerical and analytical methods we demonstrate that the multifractality of the GS is a universal property of all of them. We choose $\gamma \geqslant 0$ and $\alpha \geqslant 0$ to ensure that off-diagonal terms of Hamiltonian matrices (1) are nonpositive, which, according to the Perron-Frobenius theorem, implies that coefficients $\Psi_{\vec{\sigma}}$ in (2) for the GS wave function are non-negative. Other parameters are such that GS wave functions of the XY models

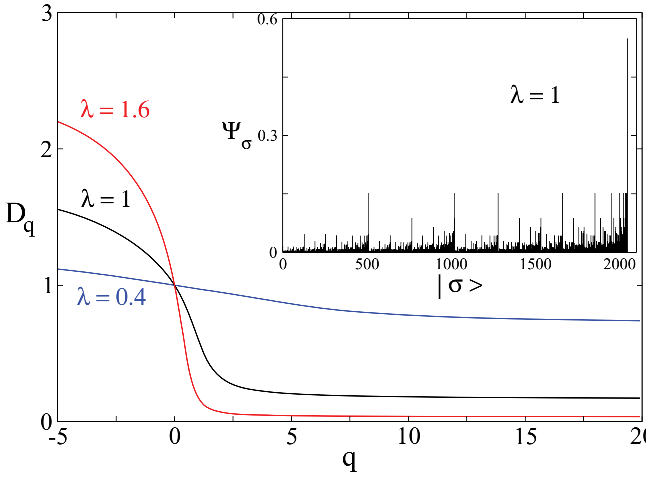

FIG. 1. (Color online) Fractal dimensions of GS for the quantum Ising model. Red line: $\lambda = 1.6$, black line: $\lambda = 1$, blue line: $\lambda = 0.4$. Inset: GS coefficients for $\lambda = 1$ and $N = 11$. The abscissa axis here and in other figures is the integer binary code for $\vec{\sigma}$, $x = \sum_{n=1}^{N} 2^{n-2}(1+\sigma_n)$.

(with $\Delta = 0$) are ferromagnetic and for the XYZ models they are antiferromagnetic.

III. QUANTUM ISING MODEL

The quantum Ising model in a transverse field [18] is a standard model of quantum phase transitions [19]. It corresponds to the Hamiltonian (1) with $\Delta = \alpha = 0$ and $\gamma = 1$. Its spectrum can be found analytically by the Jordan-Wigner transformation [3], and coefficients $|\Psi_{\vec{\sigma}}|^2$ are given by the determinant of $N \times N$ matrices [3,12].

Fractal dimensions of the GS wave function for this model computed numerically from a linear extrapolation of the Rényi entropy with $N = 3$–11 are presented in Fig. 1 for a few values of transverse field λ. The curves of D_q as a function of q for all models have the same characteristic form as for other fractal measures [7]. In particular, when $q \to \pm\infty$, they tend to well defined limits $D_{\pm\infty}$.

Generalizing the results of [12], one gets the exact expressions for limiting values $D_{\pm\infty}$ and for $D_{1/2}$,

$$D_{\pm\infty}(\lambda) = \frac{1}{2} - \frac{1}{2\pi \ln 2}\int_0^{\pi} \ln\left[1 \pm \frac{\lambda - \cos u}{\sqrt{R(\lambda,u)}}\right] du,$$
$$D_{1/2}(\lambda) = 1 - D_{\infty}\left(\frac{1}{\lambda}\right), \quad R(\lambda,u) = 1 - 2\lambda\cos u + \lambda^2. \tag{5}$$

These formulas prove that fractal dimensions of the quantum Ising model are nontrivial. In Fig. 2, these exact expressions are plotted together with numerically calculated points for different λ. $D_{\pm\infty}$ are obtained by a fit $D_{\pm\infty} + a/q + b/q^2$ for large q parts of curves similar to Fig. 1. The good agreement between Eqs. (5) and numerics shows that although we obtain fractal dimensions from a relatively small number of spins, our results are reliable.

The above curves are qualitatively the same for the noncritical and critical (that is, $\lambda = 1$) quantum Ising model. Nevertheless, as illustrated in the inset of Fig. 2, the sum of

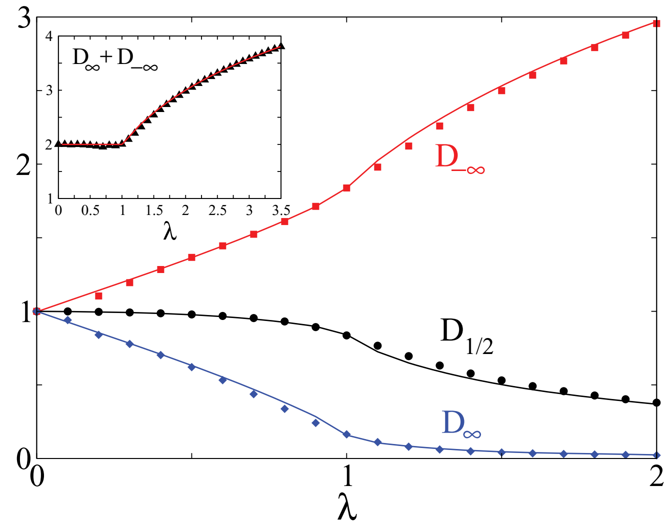

FIG. 2. (Color online) Exact fractal dimensions (5) for the quantum Ising model: D_∞ [blue (lower) line], $D_{1/2}$ [black (middle) line], and $D_{-\infty}$ [red (upper) line]. Results of numerical calculations are indicated by symbols of the same color. Inset: $D_\infty + D_{-\infty}$ calculated numerically (black triangles) in comparison with Eq. (6) (red solid line).

D_∞ and $D_{-\infty}$ has clear singularity in the critical point in accordance with the relation

$$D_{-\infty}(\lambda) + D_{\infty}(\lambda) = \begin{cases} 2, & |\lambda| < 1, \\ 2 + \frac{\ln|\lambda|}{\ln 2}, & |\lambda| > 1, \end{cases} \tag{6}$$

which follows from (5). This means that criticality can be observed in fractal dimensions of the GS.

IV. *XY* MODEL

The XY model is a specification of (1) with $\Delta = \alpha = 0$ and $\gamma \neq 1$. Similar to the quantum Ising model, this model is also integrable by the Jordan-Wigner transformation [3,12], but the structure of its GS is more complicated. An interesting special case is $\lambda = \lambda_f$, where $\lambda_f = \sqrt{1-\gamma^2}$. It is known [20] that at that field the XY model has two exact factorized GS wave functions,

$$\Psi = \prod_{n=1}^{N}(\cos\theta|1\rangle_n \pm \sin\theta|-1\rangle_n), \quad \cos^2 2\theta = \frac{1-\gamma}{1+\gamma}. \tag{7}$$

For states with definite parity and $\lambda = \lambda_f$, fractal dimensions are described by a formula

$$D_q = -\frac{\ln(\cos^{2q}\theta + \sin^{2q}\theta)}{(q-1)\ln 2} \tag{8}$$

indicated for $\gamma = 0.6$ and $\lambda = 0.8$ by the dashed black line in Fig. 3. This example proves that at least at the factorizing field, fractal dimensions of the GS wave function do exist and correspond to the well-investigated case of binomial measures [6].

As for $\lambda^2 + \gamma^2 < 1$ there exist many crossings of lowest states with different parity, for numerical calculations (performed as in the Ising model) we choose λ and γ outside the

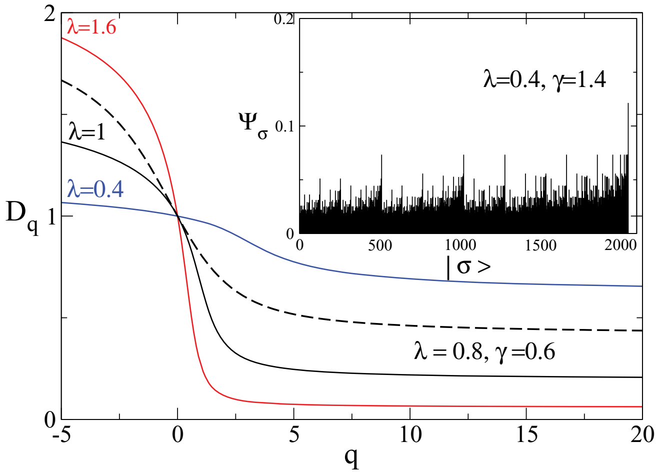

FIG. 3. (Color online) Fractal dimensions of GS for the XY model with anisotropy $\gamma = 1.4$. Red line: $\lambda = 1.6$, black line: $\lambda = 1$, blue line: $\lambda = 0.4$. Dashed black line shows for comparison the exact fractal dimensions (8) for $\lambda = 0.8$ and $\gamma = 0.6$. Inset: GS coefficients for $\lambda = 0.4$, $\gamma = 1.4$, and $N = 11$.

unit circle, $\lambda^2 + \gamma^2 > 1$. The results are presented in Fig. 3 and are qualitatively similar to the Ising model.

One may argue that the limiting values D_∞ and $D_{-\infty}$ as in the quantum Ising model should correspond to configurations with, respectively, all spins up and all spins down, and, consequently, they are expressed similar to (5) as

$$D_\pm(\lambda,\gamma) = \frac{1}{2} - \frac{1}{2\pi \ln 2}\int_0^\pi \ln\left[1 \pm \frac{\lambda - \cos u}{\sqrt{R_-(\lambda,\gamma,u)}}\right] du \quad (9)$$

with $R_-(\lambda,\gamma,u) = (\lambda - \cos u)^2 + \gamma^2 \sin^2 u$. But for small λ, the minimal contribution is instead given by the antiferromagnetic Néel configuration with alternating spins, $\sigma_n = (-1)^n$. Using the asymptotics of the block Toeplitz matrices [21], we get

$$D_{\text{Néel}}(\lambda,\gamma) = \frac{3}{4} - \frac{1}{2\pi \ln 2}\int_0^{\pi/2} \ln\left[1 - \frac{\lambda^2 + \gamma^2 - (1+\gamma^2)\cos^2 u}{\sqrt{R_+(\lambda,\gamma,u) R_-(\lambda,\gamma,u)}}\right] du, \quad (10)$$

where $R_+(\lambda,\gamma,u) = (\lambda + \cos u)^2 + \gamma^2 \sin^2 u$. This result for $\gamma = 1.4$ is presented in Fig. 4 by the black line. When $D_{\text{Néel}} > D_-$, $D_{-\infty} = D_{\text{Néel}}$, otherwise $D_{-\infty} = D_-$. For $\gamma = 1.4$, these curves intersect at $\lambda \approx 0.4982$, and $D_{-\infty}$ has the form indicated in Fig. 4 by solid blue and black lines. Numerical results agree well with this prediction.

V. ISING MODEL IN TRANSVERSE AND LONGITUDINAL FIELDS

The Ising model in transverse and longitudinal fields is obtained by adding to the quantum Ising model a longitudinal field α. For nonzero α, the only known integrable case corresponds to $\lambda = 1$ [22]. This model has recently attracted a great deal of attention as certain consequences of its integrability have been checked experimentally in the cobalt niobate ferromagnet [23]. In Fig. 5, the fractal dimensions for a few values of both fields are presented.

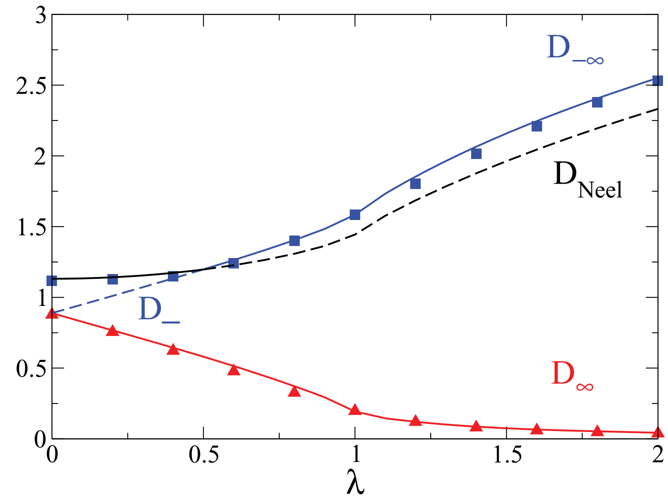

FIG. 4. (Color online) Asymptotic fractal dimensions for the XY model with anisotropy $\gamma = 1.4$ vs transverse field. Red and blue lines indicate $D_\pm$ in (9). Black line is the contribution of the Néel configuration (10). When contributions become subdominant, they are indicated by dashed lines of the same color. Blue squares and red triangles are, respectively, $D_{-\infty}$ and D_∞ calculated as for the Ising model.

VI. XXZ MODEL

The XXZ model in zero fields is a particular case of the Heisenberg model (1) with $\gamma = \lambda = \alpha = 0$ and $\Delta \neq 0$. Due to the conservation of the z component of the total spin, $S_z = \sum_n \sigma_n^z$, its Hamiltonian can be diagonalized in subspace with fixed S_z. The model is soluble by the coordinate Bethe ansatz [2,24,25] and has a rich phase diagram (see, e.g., [4]).

As a reference, we use $\Delta = -\frac{1}{2}$, called the combinatorial point. From the Razumov-Stroganov conjecture [26] proved in [27], it follows that at such Δ and odd $N = 2R + 1$ the following statements are valid: (i) the GS energy is $-3N/4$, (ii) the largest coefficient in the expansion (2) (the one for the

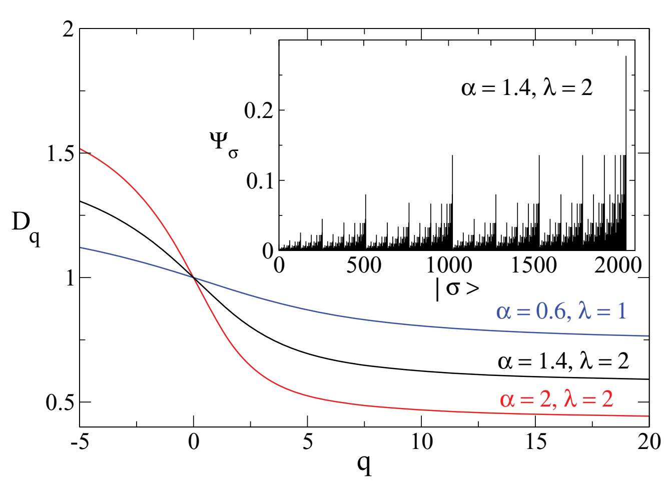

FIG. 5. (Color online) Fractal dimensions for the quantum Ising model in transverse (λ) and longitudinal (α) fields. Red line: $\alpha = 2$, $\lambda = 2$; black line: $\alpha = 1.4$, $\lambda = 2$; blue line: $\alpha = 0.6$, $\lambda = 0.4$. Inset: GS coefficients for $\alpha = 1.4$, $\lambda = 2$, and $N = 11$.

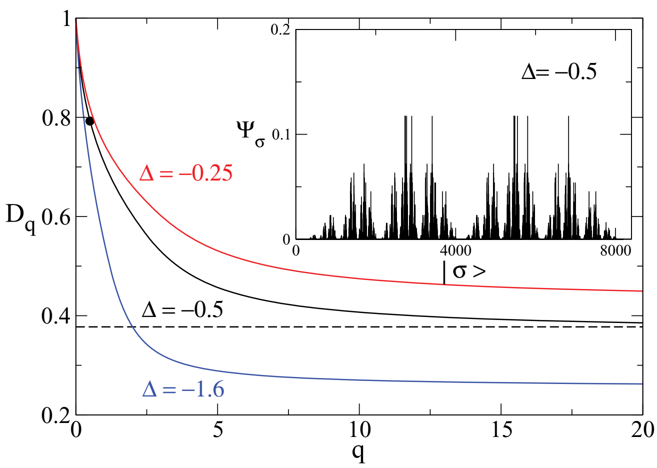

FIG. 6. (Color online) Fractal dimensions for the XXZ model in zero fields. Red line: $\Delta = -0.25$, black line: combinatorial point $\Delta = -0.5$, blue line: $\Delta = -1.6$. Inset: GS coefficients for $\Delta = -0.5$ and $N = 13$. Dashed line indicates the theoretical prediction for D_∞ (12) at $\Delta = -0.5$. Black circle is the value of $D_{1/2}$ (12) at this point.

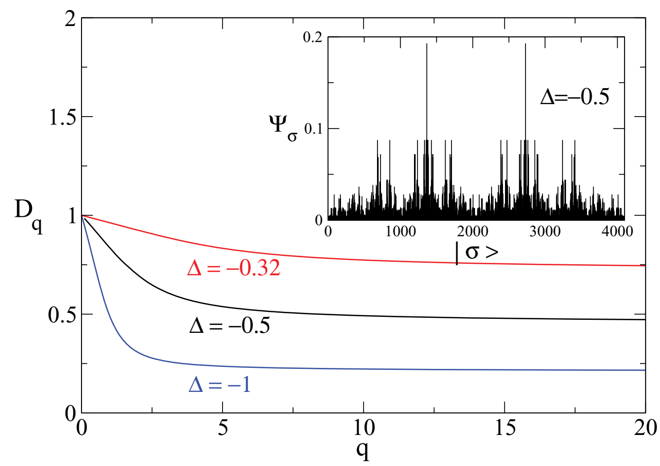

FIG. 7. (Color online) Fractal dimensions for the XYZ model with anisotropy $\gamma = 0.6$. Red line: combinatorial point $\Delta = -0.32$, black line: $\Delta = -0.5$, blue line: $\Delta = -1$. Inset: GS coefficients for $\Delta = -0.5$, $\gamma = 0.6$, and $N = 12$.

Néel configuration) equals

$$\Psi_{\rm max}^{-1} = \frac{3^{R/2}}{2^R} \frac{2 \times 5 \cdots (3R-1)}{1 \times 3 \cdots (2R-1)}\,, \tag{11}$$

(iii) the smallest coefficient corresponding to one half consecutive spins up and the other half spins down is $\Psi_{\rm min}^{-1} = \Psi_{\rm max}^{-1} A_R$, and (iv) $\sum_{\vec\sigma} \Psi_{\vec\sigma} = 3^{R/2}$. Here A_R is the number of alternating sign matrices [28].

These formulas prove that for $\Delta = -\frac{1}{2}$, fractal dimensions D_∞ and $D_{1/2}$ are explicitly known,

$$D_\infty = \frac{3 \ln 3}{2 \ln 2} - 2 \approx 0.377, \quad D_{1/2} = \frac{\ln 3}{2 \ln 2} \approx 0.792\,. \tag{12}$$

When $R \to \infty$, $\ln A_R = R^2 \ln(3\sqrt{3}/4) + O(R)$. Such quadratic in N behavior is a particular case of the emptiness formation probability of a string of n aligned spins with $n \sim N$ [29]. This asymptotics means that negative moments of the GS wave function in the antiferromagnetic case require a scaling different from (4) and hence will not be considered here. The fractal dimensions for a few values of parameter Δ are presented in Fig. 6. The numerical calculations were performed by extrapolation of the Rényi entropy separately for odd and even $N = 3$–13. With available precision, fractal dimensions for odd and even N are the same, but subleading terms in the Rényi entropy (3) are different.

VII. XYZ MODEL

The XYZ model differs from the XXZ model by anisotropy $\gamma \neq 0$ in the (x,y) plane. In zero fields, its GS wave function has been found in [5]. A soluble example with a factorized GS (7) is $\alpha = 0$, $\lambda = \lambda_f$ [20], where

$$\lambda_f = \sqrt{(1-\Delta)^2 - \gamma^2}, \quad \cos^2 2\theta = \frac{1-\gamma-\Delta}{1+\gamma-\Delta}\,. \tag{13}$$

At this field, the GS wave function corresponds to the binomial measure, and fractal dimensions are given by (8).

The combinatorial point for the XYZ model in zero fields at which additional information about the GS is known (or conjectured) is $\Delta = (\gamma^2 - 1)/2$ [30]. In Fig. 7, we present the fractal dimension in the zero-field XYZ model with $\gamma = 0.6$ for a few values of Δ including the combinatorial point. Qualitatively, the curves are similar to the XXZ model and to D_q with positive q for the XY models.

VIII. SUMMARY

We perform systematic studies of practically all standard one-dimensional spin-$\frac{1}{2}$ models and demonstrate that their ground state wave functions are multifractals in the natural spin-z basis with, in general, nontrivial fractal dimensions. For special values of parameters and/or certain dimensions, we get exact analytical formulas which prove rigorously the existence of fractal dimensions. In other cases, we rely on numerical calculations. The multifractality in spin chains is a robust and universal phenomenon. It exists for integrable and nonintegrable models, for ferromagnetic and antiferromagnetic states, as well as for critical and noncritical systems. Nevertheless, such a property is nontrivial and not automatic. If, e.g., one generates coefficients randomly, the result, in general, is not multifractal.

A common point of these models is that their $M \times M$ Hamiltonian matrix in each row and column has only $K \sim \ln M$ nonzero matrix elements of the same order. This specific form resembles a tree structure with branching number $K \ll M$. As $K \to \infty$ when $M \to \infty$ and on a tree with a large branching number (with other parameters fixed), the Anderson localization is unlikely [31,32] as states are delocalized. On the other hand, the full ergodicity on a tree is, in general, also improbable [32]. The remaining possibility corresponds to delocalized but not ergodic states, i.e., to multifractality, which may explain its ubiquity.

Multifractality in spin chains seems to be of a different origin than in the Anderson model at the MIT point [9,10] (or in critical random banded matrices which are the preferred toy models of wave function multifractality [9,33]). In such critical models, the multifractality is related to a subtle interplay between spreading and disorder (i.e., criticality). On the contrary, in spin-$\frac{1}{2}$ chains it reflects the complexity of the internal structure of 2^N-dimensional space $\{0,1\}^N$ when $N \to \infty$. The fact that explicitly known functions like (7) correspond to multifractal measures may seem strange, but properties of large-dimensional spaces are sometimes counterintuitive (see, e.g., the concentration of measure in such spaces [34]).

The above arguments are not restricted to one dimension and/or spin chains but can be applied to various many-body problems with local interactions, and we conjecture that multifractality is a generic property of a large class of such models.

ACKNOWLEDGMENTS

The authors are greatly indebted to O. Giraud and G. Roux for numerous useful comments and valuable help in performing numerical calculations. We thank B. Altschuler for fruitful discussions, O. Giraud for a careful reading of the manuscript, and G. Roux for pointing out Ref. [15]. One of the authors (Y.Y.A.) was supported by the CFM Foundation.

[1] W. Heisenberg, Z. Phys. **49**, 619 (1928).
[2] H. Bethe, Z. Phys. **71**, 205 (1931).
[3] E. Lieb, T. Schultz, and D. Mattis, Ann. Phys. (NY) **16**, 407 (1961).
[4] D. C. Mattis, *The Many Body Problem* (World Scientific, Singapore, 1994).
[5] R. J. Baxter, *Exactly Solved Models in Statistical Mechanics* (Academic, New York, 1982).
[6] B. B. Mandelbrot, *The Fractal Geometry of Nature* (Freeman, New York, 1982).
[7] T. C. Halsey, M. H. Jensen, L. P. Kadanoff, I. Procaccia, and B. I. Shraiman, Phys. Rev. A **33**, 1141 (1986).
[8] H. E. Stanley and P. Meakin, Nature (London) **335**, 405 (1988).
[9] B. I. Shklovskii, B. Shapiro, B. R. Sears, P. Lambrianides, and H. B. Shore, Phys. Rev. B **47**, 11487 (1993).
[10] A. D. Mirlin and F. Evers, Phys. Rev. B **62**, 7920 (2000).
[11] J.-M. Stéphan, S. Furukawa, G. Misguich, and V. Pasquier, Phys. Rev. B **80**, 184421 (2009).
[12] J.-M. Stéphan, G. Misguich, and V. Pasquier, Phys. Rev. B **82**, 125455 (2010); **84**, 195128 (2011).
[13] M. P. Zaletel, J. H. Bardarson, and J. E. Moore, Phys. Rev. Lett. **107**, 020402 (2011).
[14] G. Vidal, J. I. Latorre, E. Rico, and A. Kitaev, Phys. Rev. Lett. **90**, 227902 (2003); J. I. Latorre, E. Rico, and G. Vidal, Quantum. Inf. Comput. **4**, 48 (2004).
[15] J. Rodriguez-Laguna *et al.*, New J. Phys. **14**, 053028 (2012).
[16] B. B. Mandelbrot, Physica A **163**, 306 (1990).
[17] R. Riedi, J. Math. Anal. Appl. **189**, 462 (1995).
[18] P. Pfeuty, Ann. Phys. (NY) **57**, 79 (1970).
[19] S. Sachdev, *Quantum Phase Transitions* (Cambridge University Press, New York, 1999).
[20] J. Kurmann, H. Thomas, and G. Müller, Physica A **112**, 235 (1982); G. Müller and R. E. Shrock, Phys. Rev. B **32**, 5845 (1985).
[21] H. Widom, Proc. Am. Math. Soc. **50**, 167 (1975).
[22] A. B. Zamolodchikov, Int. J. Mod. Phys. **4**, 4235 (1989).
[23] R. Coldea *et al.*, Science **327**, 177 (2010).
[24] C. N. Yang and C. P. Yang, Phys. Rev. **150**, 321 (1966).
[25] R. Orbach, Phys. Rev. **112**, 309 (1958).
[26] A. V. Razumov and Yu. G. Stroganov, J. Phys. A **34**, 3185 (2001).
[27] L. Cantini and A. Sportiello, J. Comb. Theory, Ser. A **118**, 1549 (2011).
[28] D. Zeilberger, Electron. J. Comb. **3**, R13 (1996).
[29] N. Kitanine *et al.*, J. Phys. A **35**, L753 (2002); V. E. Korepin *et al.*, Phys. Lett. A **312**, 21 (2003).
[30] A. V. Razumov and Yu. G. Stroganov, Theor. Math. Phys. **164**, 977 (2010).
[31] R. Abou-Chacra, D. J. Thouless, and P. W. Anderson, J. Phys. C **6**, 1734 (1973).
[32] B. L. Altshuler, Y. Gefen, A. Kamenev, and L. S. Levitov, Phys. Rev. Lett. **78**, 2803 (1997).
[33] A. D. Mirlin, Y. V. Fyodorov, F. M. Dittes, J. Quezada, and T. H. Seligman, Phys. Rev. E **54**, 3221 (1996).
[34] D. P. Dubhashi and A. Panconesi, *Concentration of Measure for the Analysis of Randomized Algorithms* (Cambridge University Press, New York, 2009).